Published in final edited form as:
J Comp Neurol. 2008 October 10; 510(5): 508–524. doi:10.1002/cne.21804.

Localization of Kv2.2 Protein in *Xenopus laevis* Embryos and Tadpoles

NICOLE G. GRAVAGNA[1,2,*], **CHRISTOPHER S. KNOECKEL**[1], **ALISON D. TAYLOR**[1], **BARBARA A. HULTGREN**[1], and **ANGELES B. RIBERA**[1,2]

[1] Department of Physiology and Biophysics, University of Colorado Denver and Health Sciences Center, Aurora, CO 80045 USA

[2] Neuroscience Program, University of Colorado Denver and Health Sciences Center, Aurora, CO 80045 USA

Abstract

Voltage-gated potassium (Kv) channels sculpt neuronal excitability and play important developmental roles. Kv channels consist of pore-forming ⟨ and auxiliary subunits. For many Kv α-subunits, existing mRNA probes and antibodies have allowed analysis of expression patterns, typically during adult stages. Here, we focus on the Kv2.2 ⟨-subunit, for which the mRNA shows broad expression in the embryo and adult. A lack of suitable antibodies, however, has hindered detailed analysis of Kv2.2 protein localization, especially during development. We developed an antibody that specifically recognizes Kv2.2 protein in *Xenopus laevis*, a vertebrate well suited for study of early developmental stages. The Kv2.2 antibody recognized heterologously expressed Kv2.2 but not the closely related Kv2.1 protein. Immunodetection of the protein showed its presence at St 32 in ventrolateral regions of the hindbrain and spinal cord. At later stages, several sensory tissues (retina, otic and olfactory epithelia) also expressed Kv2.2 protein. As development progressed in the central nervous system, Kv2.2 protein distribution expanded in close association with the cytoskeletal marker α-tubulin, consistent with growth of neuronal tracts. We analyzed the subcellular distribution of Kv2.2 protein within single cultured neurons. In addition to a surface membrane presence, Kv2.2 protein also resided intracellularly closely associated with α-tubulin, as *in vivo*. Further, in contrast to Kv2.1, Kv2.2 protein localized to long axonal-like processes, consistent with its *in vivo* location in tracts. Despite their primary sequence similarity, the contrasting localizations of Kv2.1 and Kv2.2 support different roles for each during development and neuronal signaling.

Indexing terms

voltage-gated potassium channel; *Xenopus laevis*; embryo; spinal cord; sensory end organ

INTRODUCTION

Voltage-gated potassium (Kv) channels comprise a large family of membrane proteins that play important roles in determining membrane excitability (Coetzee et al., 1999). In the adult, individual neurons each express several different Kv channels that sculpt the characteristic excitability phenotype of the cell. While much has been learned about the

[*]Correspondence to: Nicole Gravagna, Department of Physiology & Biophysics, MS 8307, 12800 East 19th Avenue, P.O. Box 6511, Aurora, CO 80045, E-mail: nicole.gravagna@uchsc.edu, (303) 724-4520, (303) 724-4501 FAX.
Associate Editor: Dr. John Rubenstein

significance of Kv channel function in adult neurons, less is known about the roles of Kv channels during development of excitable tissues.

Molecular cloning has identified at least twelve different subfamilies of Kv α-subunit channel genes that are expressed in a variety of excitable as well as non-excitable tissues (Gutman et al., 2005). Each Kv subfamily contains several members. Individual Kv α-subunit genes encode a transmembrane protein that tetramerizes to form a single potassium channel. The Kv1 subfamily contains at least eight different members (Gutman et al., 2005). Within Kv subfamilies, additional diversity arises when subunits heteromultimerize, as has been found within the Kv1, Kv3 and Kv4 subfamilies (Shahidullah et al., 1995; Sheng et al., 1993; Song et al., 1998).

The Kv2 potassium channel subfamily has only two members, Kv2.1 (Frech et al., 1989) and Kv2.2 (Hwang et al., 1992; Burger and Ribera, 1996; Gutman et al., 2005). While Kv2.1 and Kv2.2 subunits can heteromultimerize in heterologous expression systems (Blaine and Ribera, 1998), immunocytochemical analyses of native tissues suggest that the two subunits do not heteromultimerize *in vivo* (Trimmer, 1991; Hwang et al., 1993a; Hwang et al., 1993b; Maletic-Savatic et al., 1995; Rhodes et al., 1995).

Kv2.1 and Kv2.2 were initially isolated from substantially different tissues, brain and a sensory epithelium, respectively. Frech et al. (1989) cloned Kv2.1, initially called drk1 (delayed rectifier K^+), from a rat brain cDNA library using a functional expression screen. Hwang et al. (1992) subsequently isolated Kv2.2 on the basis of homology to Kv2.1. Because Kv2.2 was cloned from a rat tongue circumvallate papillae cDNA library, it was initially called cdrk (circumvallate delayed rectifier K^+).

At the amino acid level, Kv2.1 and Kv2.2 subunits resemble each other and share 62% identity overall. However, the similarity is restricted to the transmembrane core regions (92% identity). The long carboxyl-terminal tail regions of Kv2.1 and Kv2.2 are only 35% identity. The existence of conserved and divergent regions within the amino acid sequences suggests that Kv2.1 and Kv2.2 may have both shared and specialized functions.

The available information, while limited, about Kv2.2 protein distribution supports the prediction of different functional roles for Kv2.1 and Kv2.2. In the adult, the two Kv2 isoforms display different localizations in neural tissues and sensory epithelia (Hwang et al., 1993a; Hwang et al., 1993b; Varela-Ramirez et al., 1998; Helyer et al., 2007). Moreover, when a single cell expresses both Kv2.1 and Kv2.2 proteins, the two subunits localize to different subcellular regions (Hwang et al., 1993b). No information is available about expression during embryonic stages, when potassium channels play both rapid signaling and developmental roles (Spitzer and Ribera, 1998).

Our goal was to provide needed information about Kv2.2 protein localization in a vertebrate system, *Xenopus laevis*, in which both embryonic and adult stages could be analyzed. We developed an antibody to a carboxyl-terminus region of *Xenopus* Kv2.2. We show here that this new antibody specifically recognizes Kv2.2 but not its close relative, Kv2.1. During embryonic, larval and pre-metamorphic stages, Kv2.2 protein localizes to post-mitotic cells at early stages of differentiation in ventrolateral regions of the brain and spinal cord, especially in areas associated with growing axonal tracts. Further, consistent with its isolation from sensory epithelia, we found Kv2.2 protein in the retina, inner ear, and olfactory epithelium shortly after these sensory tissues begin to form. Overall, the results indicate that many neurons and sensory cells begin to synthesize Kv2.2 protein at early stages of post-mitotic differentiation and maintain expression thereafter. Moreover, Kv2.2 is present in the axon, in contrast to the dendritic localization of Kv2.1.

MATERIALS AND METHODS

Animals

Adult *Xenopus leavis* were housed in the Center for Comparative Medicine at the University of Colorado Denver at the Anschutz Medical Center (UCD at AMC). Embryos were obtained by standard *in vitro* fertilization methods (e.g., Blaine and Ribera, 1998). All *Xenopus leavis* were handled in accordance with the Institutional Animal Care and Use Committee of UCD at AMC.

Generation of the anti-Kv2.2 Antibody

The immunogenic 26 residue peptide, corresponding to amino acids 828–853 of *Xenopus* Kv2.2 (KEKPEGHFVNLETSLLSPQKTISQN), was synthesized by Global Peptides (Fort Collins, CO); a cysteine residue was added to the carboxyl end of the sequence for coupling purposes. The Kv2.2 subunit-specific antibody was generated in rabbits by PhosphoSolutions, Inc. (Aurora, CO; www.PhosphoSolutions.com) and affinity-purified using the immunogenic peptide.

Protein extraction

Tissues were homogenized in MK lysis buffer (50mM Tris pH 8.0, 150 mM NaCl, 0.5% NP40, 0.5% Triton-X100, 1 mM EGTA; pH 7.4; Klymkowsky Lab On-line Methods) with added 1x protease inhibitor (Halt Protease Inhibitor Cocktail Kit, Pierce Chemicals, Rockford, IL).

HEK Cells

Xenopus Kv2.2 and Kv2.1 cDNAs were subcloned into the pCS2+ vector (Turner and Weintraub, 1994) that contains the CMV promoter to drive expression in mammalian cells. HEK293 cells were transfected with DNA using the Effectene transfection reagent according to the manufacturer's instructions (Qiagen Inc., Valencia, CA). Confluent transfected cells were harvested by lysis in MK buffer with freshly added protease inhibitors (5 mM NaF, 0.2 mM PMSF, 0.1 mg/mL benzamidine, 0.2 mM sodium orthovanadate, 5 mM sodium pyrophosphate, 20 mM BAPTA, and 1 μg/mL Protease Inhibitor Cocktail Set III [Calbiochem, EMD Chemicals, San Diego, CA]). Cell slurries were centrifuged and stored at −20°C.

Western blot

Protein extracts (20–100 μg) were separated on sodium dodecyl sulfate-polyacrylamide gels using electrophoresis (SDS-PAGE) and then transferred to a nitrocellulose membrane. The membrane was blocked for 30 minutes in a Tris buffered saline-Tween solution (TBST: 0.136 M NaCl, 2.68 mM KCl, 24.76 mM Tris, pH 7.4, 0.1% Tween 20) containing 5% non-fat dry milk. The membrane was then exposed for 2 hours at room temperature to the primary antibody (1:100). Membranes were washed in TBST and then exposed to the species appropriate secondary antibody conjugated to horseradish peroxidase at a concentration of 1:2000 at room temperature. The blot was washed again in TBST and developed using SuperSignal West Dura Extended Duration Substrate (Pierce Chemicals). Controls consisted of incubating lyophilized peptide (0.5 mg) with the antibody overnight before dilution and subsequent application to the blot.

Indirect immunofluorescence on cryostat sections

Whole embryos were fixed in 4% paraformaldehyde in PBS [150 mM NaCl, 2.6 mM KCl, 14.5 mM Na_2HPO_4, 14.5 mM KH_2PO_4], cryoprotected in 30% sucrose, embedded, and frozen. 18 μm transverse cryostat sections were mounted on poly-L-lysine dipped slides and

preincubated in PBSTS-BSA (PBST with 10% heat-inactivated goat serum and 0.5 μg/μl BSA) and then incubated overnight at 4°C with primary antibody (see below and Table I). After removal of the primary antibody and washes, slides were incubated overnight with secondary antibody (1:1000 Alexa 488 or Alexa 568 conjugated goat anti-rabbit; Molecular Probes-Invitrogen, Carlsbad, CA). Sections were counter-stained with Hoechst (Molecular Probes-Invitrogen) and cover-slipped with Fluormount-G (Southern Biotechnology Associates, Birmingham, Al). We also used a toxin, phalloidin (Molecular Probes) conjugated to Oregon Green 488 to label F-actin.

Antibody Characterization

Primary antibodies used in this study are listed in Table I. The Kv2.2 antibody was a rabbit polyclonal whereas the other antibodies were mouse monoclonals. Specific information about each antibody's generation and characterization is given below:

Anti-acetylated α-tubulin (aat; Sigma-Aldrich; 6–11B-1 clone; Table I)—Aat, a component of microtubules, is detected in the processes and somata of differentiating neurons of neural fold/tube stage *Xenopus* embryos (Chu and Klymkowsky, 1989). Piperno and Fuller (1985) developed the aat mouse monoclonal antibody by immunizing mice against a 15S complex of sperm axonemes prepared from *Strongylocentrotus purpuratus* (sea urchin), followed by fusion of splenocytes and myeloma cells. In Western blot, the 6-11B-1 clone recognized specifically a 55 KDa band corresponding to axonemal α-tubulin but not taxol-stabilized microtubules; the aat monoclonal recognizes aat in many different species (Piperno and Fuller, 1985).

HNK-1 (VC1.1 clone; Table I)—HNK-1, an antibody to a carbohydrate antigen bound to many neural cell adhesion molecules, localizes to somata and processes of neurons during early development of the *Xenopus* neural tube (Nordlander, 1993). Arimatsu et al. (1987) developed the HNK-1 antibody (clone VC1.1) by immunizing mice against unfixed homogenates of cat primary visual cortex, followed by fusion of splenocytes and myeloma cells. In Western blot, the VC1.1 clone recognized specifically 145 and 170 kD neural cell adhesion isoforms from rat brain (Naegele and Barnstable, 1991).

Anti-syntaxin (syn; HPC-1 clone; Table I)—The syntaxin mouse monoclonal antibody was generated by first immunizing mice with a synaptosomal plasma-membrane fraction prepared from adult rat hippocampus, and then creating hybridomas from splenocytes and myeloma cells. Previous immunoblot analysis indicated that, in extracts prepared from larval *Xenopus* olfactory bulb homogenates, HPC-1 recognized a single band of ~35 kDa consistent with the expected molecular weight for syntaxin (Manzini et al., 2007). Using HPC-1, we also detected a single band of ~35 KDa in extracts prepared from *Xenopus* adult brain and St 32 whole embryos. The syntaxin monoclonal antibody labels presynaptic proteins (Manzini et al., 2007).

3A10 (3A10; Table I)—The 3A10 mouse monoclonal antibody detects commissural interneurons in *Xenopus* embryos (Robles and Gomez, 2006). The 3A10 monoclonal antibody was generated by first immunizing mice against ventral spinal cord and assorted nervous tissue, and, then, fusing splenocytes to mouse myeloma cells. The antibody was donated to the Developmental Studies Hybridoma Bank by Dr. T.M. Jessell and J. Dodd (Columbia University, NY).

Controls—For the Kv2.2 antibody, preadsorption controls were performed by incubating the antibody with the immunogenic peptide (0.1 mg peptide/10 μl undiluted antibody) prior to use. For the other primary antibodies, we obtained patterns of cellular morphology and

labeling that were similar to those previously found for *Xenopus* embryos (aat: Chu and Klymkowsky, 1989; HNK-1: Nordlander, 1993; 3A10: Robles and Gomez, 2006; syn: Manzini et al., 2006).

Confocal laser scanning and data analysis

Confocal microscopy was performed on either a Zeiss Pascal or LSM510 Microscope (Zeiss LSM 5, Carl Zeiss Inc., Thornwood, NY) with either 10X or 63X oil immersion objectives using diode (405 nm), Argon (488 nm), and Helium-Neon (543 nm) lasers. Digital images were acquired using the Zeiss LSM Confocal Software. Images for sections stained with either Kv2.2 or preblocked Kv2.2 antibodies were acquired using the same settings. Data are presented as projections of 12–17 1 μm confocal slices; within one figure, the projections shown in different panels were made from the same number of confocal slices. Images were imported into Adobe Photoshop CS2 or Corel Painter X for preparation of figures (Adobe Photoshop version 4.0; Adobe Systems, San Jose, CA). Contrast was adjusted and images were resized equally across developmental stages within a Figure.

For calculation of immunoreactive areas, we used the Zeiss LSM5 and Slidebook 4 Digital Microscopy 4.0.10.3 software to calculate the number of pixels contained within the entire spinal cord and how many of those were Kv2.2 immunofluorescent. The data are presented as mean ± S.D. ANOVA, followed by Bonferroni correction for multiple comparisons, was used to determine the statistical significance of the differences in the means of the compared groups of data. For analysis of colocalization in individual 1 μm confocal slices, we set thresholds to background and used the Zeiss LSM software to construct scatter plots and calculate the Pearson correlation coefficient (PC; Bolte and Cordelieres, 2006). PC evaluates the correlation of the intensity distributions for the examined fluorophores and has values ranging between −1 and 1; −1 indicates a negative correlation; 0, no correlation; 1, total correlation. Values greater than 0.5 were interpreted as indicative of colocalization (Bolte and Cordelieres, 2006).

Preparation of neural plate stage cultures

Neural plates were dissected from stage (St) 15/17 embryos, and cells were dissociated non-enzymatically using standard methods (Spitzer and Lamborghini, 1976; Ribera and Spitzer, 1989). Dissociated cells were plated on poly-lysine coated glass coverslips. After 24 hr *in vitro*, cultures were fixed using 4% paraformaldehyde, washed and incubated with primary antibodies (Table 1). Primary antibody binding was revealed indirectly by use of fluorescently-labeled secondary antibodies.

Indirect immunofluorescence analysis of cultured neurons

We analyzed indirect immunofluoresence signals of cultured neurons with either epifluorescent or confocal methods. For epifluorescent examination, we used an OLYMPUS IX81 (Japan) inverted motorized microscope equipped with a TIRFM PLAN APO 60X oil objective (N.A. 1.45 WD 0.15mm) located in the Light Microscopy Facility on the Anschutz Medical Campus (Aurora, Co). Epifluorescent images were obtained using a 100 watt Hg lamp with the appropriate filter sets. We also obtained epifluorescent images using either a 488 nm argon laser and the FITC emission filter or a 543 nm Helium-Neon Laser and the TRITC emission filter. Images were recorded with a Hamamatsu ORCA ER monochromatic CCD camera (Hamamatsu Corporation, Bridgewater, NJ) through the Intelligent Imaging Slidebook v.4.0.1 acquisition software (Intelligent Imaging Innovations, Inc. Denver, CO). Confocal images were acquired as described above except that images presented single 1 μm confocal slices.

RESULTS

Anti-Kv2.2 recognized a 120 kDa protein in *Xenopus* brain tissue

To develop a Kv2.2 subunit-specific antibody, we used as an immunogen a 26-residue peptide corresponding to a region across which Kv2.2 and Kv2.1 are only 14.3% identical. We tested the efficacy and specificity of the antibody by heterologous expression in HEK cells followed by western blot analysis on membrane protein extracts. We first examined whether anti-Kv2.2 recognized any proteins endogenous to HEK cells and found that this was not the case (Fig. 1). Similarly, the antibody did not recognize protein in HEK cells transfected with Kv2.1 cDNA. In contrast, the Kv2.2 antibody detected a protein with an apparent molecular weight of 120 kDa in extracts from HEK cells transfected with Kv2.2 cDNA (Fig. 1). The lack of detection of Kv2.1 protein by the Kv2.2 antibody might have occurred if the transfection for Kv2.1 had not been successful. However, electrophysiology recordings from the Kv2.1-transfected HEK cells revealed functional expression of large amplitude delayed rectifying currents not present in untransfected HEK cells (data not shown). Thus, the Kv2.2 antibody distinguishes between Kv2.2 and the closely related subunit, Kv2.1.

In mammals, the adult brain expresses Kv2.2 protein (Hwang et al., 1992). To examine whether adult *Xenopus* brain also contains Kv2.2, we again used western blot analysis. Similarly to HEK cells transfected with Kv2.2 cDNA, *Xenopus* brain contained a 120 kDa immunoreactive protein (Fig. 1). The predicted molecular weight of Kv2.2 is 99.6 kDa. However, the Kv2.2 antibody recognized an apparent molecular weight band of 120 kDa both in native tissue (brain), and in HEK cells heterologously expressing Kv2.2. The difference between the predicted and observed molecular weights may be due to aberrant migration of Kv2.2 in SDS-PAGE or post-translation modifications such as glycosylation or phosphorylation, as noted for other Kv proteins (Brooks et al., 2006). Similar differences between the predicted and apparent molecular weights of rat Kv2.2 have been previously reported (Hwang et al., 1993b). Whatever the basis for the difference, the same modifications appear to occur heterologously as well as *in vivo*, because the antibody detected proteins of similar molecular weights in brain and Kv2.2-transfected HEK cells.

In addition to the 120 kDa band, *Xenopus* brain tissue contained prominent higher molecular weight immunoreactive bands of 240 and even higher apparent molecular weights. The functional Kv2.2 channel exists as a tetramer *in vivo*, and, as observed for other Kv subunits, the quaternary structure may persist during protein extraction (Gutman et al., 2005). Accordingly, the 240 and 480 kDa bands correspond to dimers and tetramers or the 120 kDa monomer, consistent with other tetrameric Kv proteins studied by western blot (Robinson and Deutsch, 2005). In addition, a faint smaller molecular weight doublet, between 48 and 50 kDa, was recognized by the antibody. Detection of all bands was blocked by pre-incubation with the epitope-specific peptide suggesting that the lower molecular weight bands arose from proteolysis (Fig. 1). Similarly sized lower molecular weight forms have been detected in rat brain by polyclonal and monoclonal antibodies recognizing mammalian Kv2.2 antibody (Hwang et al., 1993b; http://www.neuromab.org/K37_89.pdf).

Kv2.2 protein was present during early stages of spinal cord development

We performed immunohistochemistry on cryostat sections of St 20 – 50 *Xenopus* embryos. Our first immunohistochemical analyses focused on the embryonic spinal cord where Kv2.2 mRNA is detected by St 23 in the ventral horn (Burger and Ribera, 1996). At St 20, Kv2.2 immunoreactivity was comparable to or barely above background (Fig. 2A). By St 32, Kv2.2 protein was consistently detected in ventrolateral regions of the spinal cord (Fig. 2B), which is the domain of Kv2.2 mRNA expression (Burger and Ribera, 1996). Further, the

protein distribution resembled that of a back-filled motor neuron in a St 35 embryo (Fig. 2C; Roberts and Clark, 1982), suggesting that the Kv2.2 localized to the soma and developing processes of motor neurons.

Similar to the mRNA expression pattern, the domain of Kv2.2 protein expanded with development. Kv2.2 immunoreactivity predominated in the most lateral regions where axonal tracts begin to form during premetamorphic stages (Fig. 2; Burger and Ribera, 1996). Between St 20 and 50, the cross-sectional area of spinal cord that was immunopositive for Kv2.2 increased from 2.2 ± 0.1 to 54.1 ± 4.2 % ($p<0.001$; Fig. 2J).

Next, we compared the localization of Kv2.2 protein in spinal cord sections to that of syntaxin (syn, a synaptic vesicle protein) and acetylated α-tubulin (aat; a cytoskeletal component; Table I; Fig. 3). At St 41, Kv2.2 immunofluorescence colocalized with syn labeling (Fig. 3; Fig. 4, PC=0.77 ± 0.04, n=8). At St 44–50, colocalization of the two signals persisted (Fig. 3), but with a weaker correlation (Fig. 4: St 44, 0.62 ± 0.02, n=5; St 50, 0.62 ± 0.05, n=12).

For aat, strong colocalization with Kv2.2 was present at St 41 (Fig. 3; Fig. 4, PC= 0.70 ± 0.04, n=20). However, at St 44 and 50, the Kv2.2 and aat immunofluorescent signals showed less colocalization (Fig. 3) as assessed by PC values near or less than 0.5 (Fig. 4I: St 44, 0.53 ± 0.03 n=4; St 50, 0.50 ± 0.04, n=16). In contrast, Kv2.2 did not colocalize with actin, another cytoskeletal protein (Fig. 4G-I, PC=0.26 ± 0.05, n=15).

We also examined the relative distributions of Kv2.2 versus 3A10 and HNK-1 immunoreactivities (Fig. 5). In *Xenopus*, the 3A10 monoclonal reveals axons of spinal commissural interneurons (Robles and Gomez, 2006). We found little colocalization between Kv2.2 and 3A10 immunoreactivities in the floor plate where the axons of commissural interneurons cross the spinal cord (Fig. 4F, I: PC=0.32 ± 0.09, n=24). In particular, in the floor plate where commissural interneuron axons cross, Kv2.2 and 3A10 labelings were clearly not overlapping (Fig. 5C, asterisks). In contrast, Kv2.2 showed colocalization with HNK-1 (Fig. 4E, I: PC=0.58 ± 0.03, n=25; Fig. 5F, arrows), a marker of glycoproteins in the plasma membrane of neurons (Nordlander, 1993). However, HNK-1 was also present in neurons devoid of Kv2.2 (Fig. 5F, arrowheads).

Kv2.2 immunoreactivity was present in the developing retina

Because the original Kv2.2 clone originated from a sensory epithelium cDNA library, we extended our analysis to include sensory tissues (retina, otic vesicle, and olfactory epithelium) that have been well characterized during premetamorphic stages of *Xenopus* development. Our analyses focused on St 41–50, when sensory tissues are relatively well-formed.

In the St 41 retina, Kv2.2 protein was prominent in the optic nerve and inner and outer plexiform layers (Fig. 6A, B). By St 44, labeling in the inner plexiform layer was still present but less pronounced (Fig. 6C). In contrast, Kv2.2 immunoreactivity in the outer plexiform layer was stronger than at St 41. Adjacent to the outer plexiform layer, photoreceptor cell bodies also displayed Kv2.2 immunoreactivity (Fig. 6C). Strong immunoreactivity persisted in the photoreceptor cell bodies to St 50, the oldest stage examined (Fig. 6D, E, F).

In the St 47 outer and inner plexiform layers, ganglion cell layer and optic nerve (Fig. 7A-C), Kv2.2 immunoreactivity overlapped with α-tubulin labeling. Within photoreceptors, however, aat and Kv2.2 displayed minimal colocalization (Fig. 7A-C). Kv2.2

immunolabeling was detected both proximal and distal to the soma, while aat showed at best a weak signal.

F-actin formed a longitudinally running network in the lens (Fig. 7E, F). F-actin was also abundant in the inner and outer plexiform and ganglion cell layers (Fig. 7E, F). However, even though Kv2.2 was also present in the outer plexiform layer, it did not colocalize with F-actin (Fig. 7F). In the photoreceptors, F-actin predominated in calycyl process-inner segment cables (Hale et al., 1996) that had distinctly separate locations from the Kv2.2 labeling present near the soma and in the inner segment (Fig. 7 D-I).

The data indicate that, as in the spinal cord, Kv2.2 protein expression initiated early during post-mitotic differentiation of several different retinal cell types and was maintained at subsequent stages. Moreover, Kv2.2 protein was prominent in the axons of retinal ganglion cells, similar to Kv2.2 presence in growing axonal tracts in the spinal cord.

Otic epithelia first expressed Kv2.2 protein during early post-mitotic stages

Kv2.2 protein was detected in the ventromedial epithelium at St 41, the site of the emerging sacculus (Fig. 8A, B) (Quick and Serrano, 2005; 2007). At St 41, Kv2.2 protein was also detected in the spiral ganglion (Fig. 8A, B), which contains the cell bodies of neurons supplying afferent innervation to the otic epithelia. The innervating nerve also displayed Kv2.2 immunoreactivity (arrowheads, Fig. 8A, B). Kv2.2 protein expression persisted in these regions to the latest stage examined, St 50. At St 50, we also detected Kv2.2 immunoreactivity in later forming semicircular canals (asterisks, Fig. 8E, F). In cells of the semicircular canals, Kv2.2 displayed an apical localization.

These data also indicated that Kv2.2 immunoreactivity was present in the hindbrain (Fig. 8A, C, E), consistent with the mRNA expression pattern reported by Burger and Ribera (1996). Kv2.2 immunoreactivity localized to ventral lateral regions, similar to its location in the spinal cord (Figs. 2, 3, 5).

In individual cells of the saccular epithelium, Kv2.2 protein predominated at apical sites (Fig. 8F inset; Fig. 9A, D, G, J), near the α-tubulin positive kinocilium (arrows, Fig. 9A-C, G-I) and the F-actin containing stereocilia (arrow, Fig. 9D-F, J-L). In addition, Kv2.2 protein was also detected along the long axis of hair cells flanking the soma.

Kv2.2 was detected in a chemosensory organ, the olfactory epithelium

Kv2.2 was first isolated from the chemosensory epithelium of the mammalian circumvallate papilla (Hwang et al., 1993a). Catfish taste buds also expressed a potassium channel gene, with a primary sequence equally similar to that of Kv2.1 and Kv2.2 (Kang et al., 2001). While we detected Kv2.2 in cells lining the mouth, tongue, and gill rakers (data not shown), the limited information available about the epithelia of the gustatory system in *Xenopus laevis* hindered analysis of oral chemosensory organs. However, more is known about the chemosensory olfactory epithelium (for review, Reiss and Burd, 1997). In premetamorphic tadpoles, the olfactory epithelia are found in the principal cavity and the vomeronasal organ. We focused on the epithelium facing the principal cavity.

At St. 47, Kv2.2 protein displayed a broad distribution in the olfactory epithelium (Fig. 10). Olfactory epithelial cells bear either cilia (aat positive) or microvilli (F-actin containing). Consistent with findings in other cells, Kv2.2 protein showed strong co-localization with aat (Fig. 10D) but not F-actin (Fig. 10A, C). Interestingly, Kv2.2 protein was detected with aat in cilia (Fig. 10D).

Kv2.2 protein localized to distal processes of individual neurons

Kv2.1 protein localizes to the soma and dendritic compartments of neurons (Lim et al., 2000). *In vivo*, we found that Kv2.2 protein also localized to the cell body region of neurons. However, in contrast to Kv2.1, we also detected Kv2.2 protein in axons (e.g., Figs. 2, 6, 9). To examine in more detail the subcellular location of Kv2.2 protein, we analyzed Kv2.2 immunoreactivity in isolated neurons in culture (Fig. 11).

Neurons were identified on the basis of morphological criteria. Further, all morphologically identified neurons expressed aat, confirming the identification criteria. The majority (99%) of aat positive neurons in culture also expressed Kv2.2 protein, consistent with the broad central nervous system distribution of Kv2.2 protein *in vivo*. Further, within individual neurons, the pattern of Kv2.2 protein distribution resembled that of aat, suggesting association of Kv2.2 containing vesicles with the microtubular cytoskeleton (Fig. 11). Consistent with the *in vivo* location of Kv2.2 protein, we found Kv2.2 protein in the cell body and processes of neurons in culture. The majority of neurons displayed Kv2.2 immunoreactivity in a long axon-like processes (Fig. 11, 12). At several positions along the long process as well as in the cell body, the Kv2.2 and aat immunofluorescence intensities were closely matched (Fig. 12).

DISCUSSION

Our findings provide new information about the developmental expression and localization of Kv2.2 protein in vertebrates. We detected widespread expression of Kv2.2 protein, both in the central nervous system, and in primary sensory tissues such as the retina and epithelia of the otic vesicle and nares. In the central nervous system, Kv2.2 expression was most prominent in ventral regions, suggesting roles in processing of sensori-motor motor information. A consistent finding for both central nervous system and sensory tissues was that cells initiated expression of Kv2.2 protein during early post-mitotic differentiation. For example, in the spinal cord, the most medial proliferative zones were consistently devoid of Kv2.2 immunoreactivity. In contrast, Kv2.1 protein has been detected in proliferating cells (Suzuki and Takimoto, 2004). Further, even though cells initiated expression of Kv2.2 protein during early stages of post-mitotic differentiaton, expression was maintained up to the latest stages examined. This finding suggests that Kv2.2 channels play important roles both during development as well as in the adult in processing of both sensory and motor information.

Developmental regulation of Kv2.2 in the spinal cord

Kv2.2 channels play a role in the developmentally-regulated increase in potassium current density that drives the shortening of the action potential duration in *Xenopus* primary spinal neurons between St 20 and 37 (Burger and Ribera, 1996; Gurantz et al., 1996; Blaine and Ribera, 2001). Our previous work, however, focused on either mRNA expression or potassium currents but not Kv2.2 protein directly. Data presented here indicate that between St 20 and 37, the percent cross-sectional spinal cord area that was Kv2.2-immunopositive increased ~10-fold (Fig. 2). Moreover, In St 23 whole mount preparations, Burger et al. (1996) detected Kv2.2 transcripts in the brain, primary neurons of the embryonic spinal cord, and embryonic myocytes. By St 35, Burger et al. (1996) found continued expression of Kv2.2 mRNA in somites, brain and spinal cord. Examination of the spinal cord *in situ* signal in tissue sections indicated that St 23 embryos expressed Kv2.2 mRNA in a larger portion of the ventrolateral spinal cord than did St 35 embryos, consistent with the expansion that we found for Kv2.2 immunolabeling in the spinal cord during this developmental period (Fig. 2).

The different methods used to assess developmental changes in potassium current (electrophysiology versus mRNA and protein studies) influence the types of comparisons that can be drawn between the data sets. For example, the electrophysiological data primarily reflected somatic currents (e.g., Blaine and Ribera, 2001), because recordings were made from cells with short or severed processes to improve the space clamp of membrane voltage. In this regard, the somatic localization of Kv2.2 protein is especially relevant. In addition, the previous mRNA and electrophysiological studies were limited to ~St 20–37, corresponding to the developmental period when changes in action potential waveform occur. With these caveats in mind, the data presented here support the view that Kv2.2 channels play a role in the developmental changes in excitability that occur in ventral but not dorsal spinal neurons.

By comparing the distribution of Kv2.2 protein to that of other markers, our data suggest that during earlier stages (e.g., St 41), a substantial portion of Kv2.2 resided intracellularly, presumably trafficking along the tubulin cytoskeleton (e.g., Figs. 3, 4, 12). By St 50, however, when process outgrowth has diminished and stable connections are established, less Kv2.2 immunoreactivity colocalized with tubulin, supporting the view that the earlier intracellular presence of Kv2.2, especially in axons, reflected trafficking to more distal portions of the axon.

The distribution of Kv2.1 protein in adult rat spinal cord contrasts significantly with what we found for Kv2.2 in pre-metamorphic *Xenopus*. In comparison to Kv2.2, Kv2.1 showed a much more restricted pattern and immunoreactivity was present in motor neurons but not in Renshaw interneurons (Muennich and Fyffe, 2004). In addition, in motor neurons, Kv2.1 immunoreactivity appeared in surface membrane clusters that were apposed to excitatory but not inhibitory presynaptic terminals, suggesting a specific function in modulating excitation of motor neurons. In contrast, we did not observe any evidence for surface membrane somatodendritic Kv2.2 clusters. Moreover, we detected Kv2.2 protein in axons, suggesting a role in intraneuronal excitability and forward transmission of neuronal signals.

Sensory organs and Kv2.2 protein

We examined the distribution of Kv2.2 protein in the retina and otic and olfactory epithelia because (1) these organs have been relatively well-characterized in premetamorphic *Xenopus* tadpoles, (2) previous work has analyzed the distribution of other potassium channels in the retina and otic epithelium (Pollock et al., 2002; Serrano et al., 2001), and (3) Kv2.2 and Kv2.1 channel distribution has been characterized in these tissues in adult mammals (Hwang et al., 1993a; Hwang et al., 1993b; Hwang et al., 1992; Trimmer, 1991), allowing important comparisons. In the retina and inner ear, we detected Kv2.2 protein in photoreceptors and hair cells, respectively, the cell types that transduce sensory information into electrical signals. In the otic epithelia, Kv2.2 was detected in ciliated cells and potentially present in ciliated receptor neurons. Overall the data suggest that Kv2.2 channels contribute to the function of cells that serve as the initial detectors of sensory information.

Retina—Kv2.2 mRNA was previously detected in the developing eye primordia of *Xenopus* embryos (Burger and Ribera, 1996). Here, we report that Kv2.2 protein localized to photoreceptors, the synaptic outer and inner plexiform layers, subsets of cells of the inner nuclear and retinal ganglion cell layers and the optic nerve (Fig. 6, 7). In the outer plexiform layer, the Kv2.2 protein was detected in the presynaptic region of photoreceptors and also present in cells opposing photoreceptors, and thus likely to be present post-synaptically as well.

The distribution of Kv2.2 protein differed substantially from those previously reported for Kv1.3, Kv1.5, Kv3.4 and Kv4.2 channels in the *Xenopus* retina (Pollock et al., 2002).

Further, Kv2.2 showed strong colocalization of Kv2.2 with aat and was not detected in the ciliary marginal zone or a radial pattern, consistent with expression in post-mitotic neurons but not Müller cells. Kv1.3, Kv1.5, Kv3.4 and Kv4.2 were detected in all or a subset of retinal ganglion cells, either in the cell body or optic nerve. In addition to being present in retinal ganglion cells, Kv1.5 was also detected in the proliferative ciliary marginal zone, unlike Kv2.2. Of the previously studied potassium channels, Kv1.3 showed the most similar distribution being present in the inner and outer plexiform layers and the optic nerve (Pollock et al., 2002). However, Kv1.3 was not detected in photoreceptors nor were Kv1.1, Kv1.3, Kv1.5., Kv3.4 or Kv4.2. These considerations suggest that each of these potassium currents plays a different role in the retina, not only because their encoded structures differ but also because of their unique characteristic locations throughout the retina.

In the adult mammalian retina, Kv2.1 protein localized to many of the sites where we detected Kv2.2 in the tadpole retina (e.g., photoreceptor inner segments, outer plexiform layer, amacrine cell processes, and ganglion cells) (Hwang et al., 1993a). However, in the adult mammal, Kv2.2 was found in the Müller cells, particularly in the endfeet. The contrasting distributions of Kv2.2 in the *Xenopus* versus mammalian retina may reflect species and/or developmental differences.

Otic epithelium—Varela-Ramirez et al. (1998) detected expression of Kv2.2 transcripts by RT-PCR in mRNA isolated from the inner ear of post-metamorphic *Xenopus laevis.* By *in situ* hybridization, Burger and Ribera (1996) observed Kv2.2 mRNA in the developing otic pit (~St 26). Consistent with these data, we detected Kv2.2 protein in otic epithelia during stages when the otic vesicle, pars inferior, endolymphatic duct, spiral ganglion, and stereocilia bundles begin to emerge (Quick and Serrano, 2005). Kv2.2 was present in spiral ganglion neurons and their axons that innervated the otic epithelia (Fig. 8). In addition, Kv2.2 localized to the apical regions of post-mitotic hair cells, just proximal to the stereocilia and kinocilia (Figs. 8, 9). In regenerating mammalian hair cells, Kv2.1 was found in a basolateral location while Kv1.3 was detected near the cuticular plate, similar to what we found for Kv2.2 (Helyer et al., 2007).

Olfactory epithelium—By whole-mount *in situ* hybridization, Burger and Ribera (1996) detected Kv2.2 mRNA in the developing olfactory pit. Consistent with the previously reported abundance of mammalian Kv2.2 protein in the circumvallate papilla, we detected strong Kv2.2 immunoreactivity in another chemosensory organ - the olfactory epithelium of premetamorphic *Xenopus* tadpoles (Fig. 10). In this tissue, Kv2.2 colocalized with cilia indicating a presence in ciliated cells of the epithelium. In rat, Kv2.2 was detected in the cell bodies of mature olfactory receptor cells (Hwang et al., 1993a).

SUMMARY

Our analysis of Kv2.2 protein reveals a broad and widespread distribution in the CNS and several sensory tissues. Further, within a neuron, Kv2.2 localizes to the soma, dendrites as well as the axon and is not restricted to any specific compartment. Kv2.2 shows different distributions both with respect to cell type as well as subcellularly in different neuronal compartments. This distribution differs from that noted for Kv2.1 protein, which is present in a smaller repertoire of neurons and restricted subcellularly to somatodendrtic regions (Hwang et al., 1993a; Maletic-Savetic et al., 1995; Muennich and Fyffe, 2004). Overall, the results support the view that Kv2.1 and Kv2.2 proteins play substantially different roles, primarily because they localize differently in the nervous system rather than because of intrinsic differences in biophysical properties.

Acknowledgments

We thank Clint Cave for advice regarding colocalization studies and comments on the manuscript; John Knoeckel for comments on the manuscript; Steve Fadul for assistance with microscopy; Dr. Anne Hansen for discussion regarding sensory epithelia; Dr. Lee Niswander for use of a cryostat.

Grant Sponsor: National Institutes of Health (NIH); Grant number, T32 HD041697 (NGG) and RO1 NS25217 and P30 NS048154 (ABR).

Abbreviations

aat	acetylated α-tubulin
ap	apical
cc	central canal
cdrk	circumvallate delayed-rectifier K^+
dh	dorsal horn
drk1	delayed-rectifier K^+ 1
fp	floor plate
gcl	ganglion cell layer
inl	inner nuclear layer
ipl	inner plexiform layer
kc	kinocilium
Kv	voltage-gated potassium
le	lens
myo	myocyte
nc	notocord
on	optic nerve
opl	outer plexiform layer
ov	otic vesicle
PC	Pearson’s correlation coefficient
rp	roof plate
sc	spinal cord
sg	spiral ganglion
St	stage
stc	stereocilia
syn	syntaxin
un	morphologically undifferentiated cell
vh	ventral horn

LITERATURE CITED

Blaine JT, Ribera AB. Heteromultimeric potassium channels formed by members of the Kv2 subfamily. J Neurosci. 1998; 18:9585–9593. [PubMed: 9822719]

Blaine JT, Ribera AB. Kv2 channels form delayed-rectifier potassium channels *in situ*. J Neurosci. 2001; 21:1473–1480. [PubMed: 11222637]

Bolte S, Cordelieres FP. A guided tour into subcellular colocalization analysis in light microscopy. J Micros. 2006; 224:213–232.

Brooks NL, Corey MJ, Schwalbe RA. Characterization of N-glycosylation consensus sequences in the Kv3.1 channel. FEBS J. 2006; 273:3287–3300. [PubMed: 16792699]

Burger C, Ribera AB. *Xenopus* spinal neurons express Kv2 potassium channel transcripts during embryonic development. J Neurosci. 1996; 16:1412–1421. [PubMed: 8778292]

Chu DT, Klymkowsky MW. The appearance of acetylated alpha-tubulin during early development and cellular differentiation in Xenopus. Dev Biol. 1989; 136:104–117. [PubMed: 2680681]

Coetzee WA, Amarillo Y, Chiu J, Chow A, Lau D, McCormack T, Moreno H, Nadal MS, Ozaita A, Pountney D, Saganich M, Vega-Saenz de Miera E, Rudy B. Molecular diversity of K^+ channels. Ann N Y Acad Sci. 1999; 868:233–285. [PubMed: 10414301]

Frech GC, VanDongen AM, Schuster G, Brown AM, Joho RH. A novel potassium channel with delayed rectifier properties isolated from rat brain by expression cloning. Nature. 1989; 340:642–645. [PubMed: 2770868]

Gurantz D, Ribera AB, Spitzer NC. Temporal regulation of Shaker- and Shab-like potassium channel gene expression in single embryonic spinal neurons during K^+ current development. J Neurosci. 1996; 16:3287–3295. [PubMed: 8627366]

Gutman GA, Chandy KG, Grissmer S, Lazdunski M, McKinnon D, Pardo LA, Robertson GA, Rudy B, Sanguinetti MC, Stuhmer W, Wang X. International Union of Pharmacology. LIII. Nomenclature and molecular relationships of voltage-gated potassium channels. Pharmacol Rev. 2005; 57:473–508. [PubMed: 16382104]

Hale IL, Fisher SK, Matsumoto B. The actin network in the ciliary stalk of photoreceptors functions in the generation of new outer segment discs. J Comp Neurol. 1996; 376:128–142. [PubMed: 8946288]

Helyer R, Cacciabue-Rivolta D, Davies D, Rivolta MN, Kros CJ, Holley MC. A model for mammalian cochlear hair cell differentiation *in vitro*: effects of retinoic acid on cytoskeletal proteins and potassium conductances. Eur J Neurosci. 2007; 25:957–973. [PubMed: 17331193]

Hwang PM, Cunningham AM, Peng YW, Snyder SH. CDRK and DRK1 K^+ channels have contrasting localizations in sensory systems. Neuroscience. 1993a; 55:613–620. [PubMed: 8413924]

Hwang PM, Fotuhi M, Bredt DS, Cunningham AM, Snyder SH. Contrasting immunohistochemical localizations in rat brain of two novel K^+ channels of the Shab subfamily. J Neurosci. 1993b; 13(4):1569–1576. [PubMed: 8463836]

Hwang PM, Glatt CE, Bredt DS, Yellen G, Snyder SH. A novel K^+ channel with unique localizations in mammalian brain: molecular cloning and characterization. Neuron. 1992; 8:473–481. [PubMed: 1550672]

Kang J, Teeter JH, Brazier SP, Nguyen ND, Chang CC, Puchalski RB. Molecular cloning and functional characterization of a novel delayed rectifier potassium channel from channel catfish (*Ictalurus punctatus*): expression in taste buds. J Neurochem. 2001; 76:1465–1474. [PubMed: 11238731]

Lim ST, Antonucci DE, Scannevin RH, Trimmer JS. A novel targeting signal for proximal clustering of the Kv2.1 K+ channel in hippocampal neurons. Neuron. 2000; 25:385–397. [PubMed: 10719893]

Maletic-Savatic M, Lenn NJ, Trimmer JS. Differential spatiotemporal expression of K^+ channel polypeptides in rat hippocampal neurons developing in situ and in vitro. J Neurosci. 1995; 15:3840–3851. [PubMed: 7751950]

Manzini I, Heermann S, Czesnik D, Brase C, Schild D, Rössler W. Presynaptic protein distribution and odour mapping in glomeruli of the olfactory bulb of *Xenopus laevis* tadpoles. Eur J Neurosci. 2007; 26:925–934. [PubMed: 17666078]

Muennich EA, Fyffe RE. Focal aggregation of voltage-gated, Kv2.1 subunit-containing, potassium channels at synaptic sites in rat spinal motoneurones. J Physiol. 2004; 554:673–685. [PubMed: 14608003]

Nordlander RH. Cellular and subcellular distribution of HNK-1 immunoreactivity in the neural tube of *Xenopus*. J Comp Neurol. 1993; 335:538–551. [PubMed: 7693773]

Piperno G, Fuller MT. Monoclonal antibodies specific for an acetylated form of α-tubulin recognize the antigen in cilia and flagella from a variety of organisms. J Cell Biol. 1985; 101:2085–2094. [PubMed: 2415535]

Pollock NS, Ferguson SC, McFarlane S. Expression of voltage-dependent potassium channels in the developing visual system of *Xenopus laevis*. J Comp Neurol. 2002; 452:381–391. [PubMed: 12355420]

Quick QA, Serrano EE. Inner ear formation during the early larval development of *Xenopus laevis*. Dev Dyn. 2005; 234:791–801. [PubMed: 16217737]

Quick QA, Serrano EE. Cell proliferation during the early compartmentalization of the *Xenopus laevis* inner ear. Int J Dev Biol. 2007; 5:201–209. [PubMed: 17486540]

Reiss JO, Burd GD. Cellular and molecular interactions in the development of the *Xenopus* olfactory system. Semin Cell Dev Biol. 1997; 8:171–179. [PubMed: 15001093]

Rhodes KJ, Keilbaugh SA, Barrezueta NX, Lopez KL, Trimmer JS. Association and colocalization of K^+ channel alpha- and beta-subunit polypeptides in rat brain. J Neurosci. 1995; 15:5360–5371. [PubMed: 7623158]

Ribera AB, Spitzer NC. A critical period of transcription required for differentiation of the action potential of spinal neurons. Neuron. 1989; 2:1055–1062. [PubMed: 2483107]

Roberts A, Clarke JD. The neuroanatomy of an amphibian embryo spinal cord. Philos Trans R Soc Lond B Biol Sci. 1982; 296:195–212. [PubMed: 17506218]

Robinson JM, Deutsch C. Coupled tertiary folding and oligomerization of the T1 domain of Kv channels. Neuron. 2005; 45:223–232. [PubMed: 15664174]

Robles E, Gomez TM. Focal adhesion kinase signaling at sites of integrin-mediated adhesion contrls axon pathfinding. Nat Neurosci. 2006; 9:1274–1283. [PubMed: 16964253]

Serrano EE, Trujillo-Provencio C, Sultemeier DR, Bullock WM, Quick QA. Identification of genes expressed in the *Xenopus* inner ear. Cell Mol Biol. 2001; 47:1229–1239. [PubMed: 11838972]

Shahidullah M, Hoshi N, Yokoyama S, Higashida H. Microheterogeneity in heteromultimeric assemblies formed by Shaker (Kv1) and Shaw (Kv3) subfamilies of voltage-gated K^+ channels. Proc Biol Sci. 1995; 261:309–317. [PubMed: 8587873]

Sheng M, Liao YJ, Jan YN, Jan LY. Presynaptic A-current based on heteromultimeric K^+channels detected *in vivo*. Nature. 1993; 365:72–75. [PubMed: 8361540]

Song WJ, Tkatch T, Baranauskas G, Ichinohe N, Kitai ST, Surmeier DJ. Somatodendritic depolarization-activated potassium currents in rat neostriatal cholinergic interneurons are predominantly of the A type and attributable to coexpression of Kv4.2 and Kv4.1 subunits. J Neurosci. 1998; 18:3124–3137. [PubMed: 9547221]

Spitzer NC, Lamborghini JE. The development of the action potential mechanism of amphibian neurons isolated in culture. Proc Natl Acad Sci U S A. 1976; 73:1641–1645. [PubMed: 1064036]

Spitzer NC, Ribera AB. Development of electrical excitability in embryonic neurons: mechanisms and roles. J Neurobiol. 1998; 37:190–197. [PubMed: 9777741]

Suzuki T, Takimoto K. Selective expression of HERG and Kv2 channels influences proliferation of uterine cancer cells. Int J Oncol. 2004; 25:153–159. [PubMed: 15202000]

Trimmer JS. Immunological identification and characterization of a delayed rectifier K^+channel polypeptide in rat brain. Proc Natl Acad Sci U S A. 1991; 88:10764–10768. [PubMed: 1961744]

Turner DL, Weintraub H. Expression of achaete-scute homolog 3 in *Xenopus* embryos converts ectodermal cells to a neural fate. Genes Dev. 1994; 8:1434–1447. [PubMed: 7926743]

Varela-Ramirez A, Trujillo-Provencio C, Serrano EE. Detection of transcripts for delayed rectifier potassium channels in the *Xenopus laevis* inner ear. Hear Res. 1998; 119:125–134. [PubMed: 9641325]

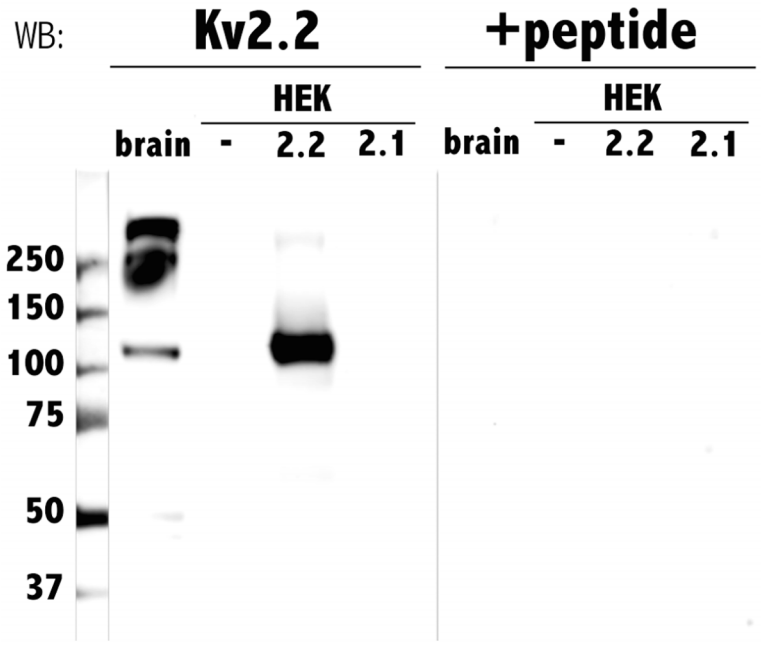

Fig. 1.

Anti-*Xenopus* Kv2.2 specifically recognized both heterologously expressed and native Kv2.2. Protein extracts from *Xenopus laevis* adult brain tissue (brain), untransfected HEK cells (−), HEK cells transfected with Kv2.2 (2.2), and HEK cells transfected with Kv2.1 (2.1) were electrophoretically separated on SDS-polyacrylamide gels, transferred to nitrocellulose membranes and incubated with either Kv2.2 antibody (left lanes, **Kv2.2**) or preblocked Kv2.2 antibody (right lanes, **+peptide**). Numbers on the left indicate the molecular weights of co-run standards.

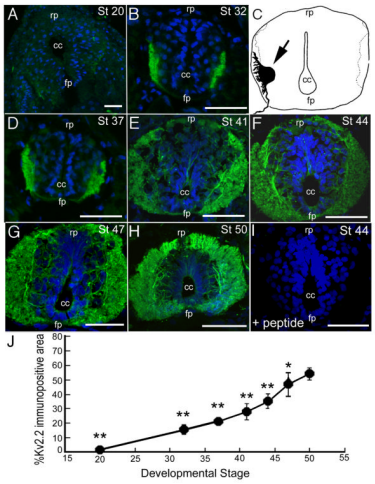

Fig. 2.

In the spinal cord, Kv2.2 immunoreactivity was detected during early stages of post-mitotic neuronal differentiation. Transverse cryostat (18 μm) sections of St 20–50 *Xenopus* embryos and tadpoles were incubated with the Kv2.2 antibody or pre-blocked Kv2.2 antibody (e.g., Panel **I**). Sections were counterstained with Hoechst (blue). In all panels, dorsal is up. cc, central canal; rp, roof plate; fp, floor plate. **A**: At St 20, Kv2.2 immunolabeling was comparable to or barely above background. **B, C, D**: Kv2.2 immunoreactivity in the St 32 (**B**) and 37 (**D**) resembled a camera lucida imag0e of a retrogradely labeled motor neuron (**C**, arrow) in the spinal cord of a St 35/36 *Xenopus* embryo (Roberts and Clarke, 1982; adapted with permission). Comparison of the motor neuron cell body in **C** to the immunoreactive signals in **B** and **D** suggested that Kv2.2 immunoreactive protein localized to both the somata and dendrites of primary spinal motor neurons. **E, F, G, H**: Between St 41–50, the Kv2.2 immunopositive region of ventrolateral spinal cord progressively expanded, consistent with growth of neuronal processes. **I**: Pre-incubation of the Kv2.2 antibody with Kv2.2 peptide (see Materials and Methods) blocked the immunoreactive signal. **J**: The percent of spinal cord cross-sectional area positive for Kv2.2 immunoreactivity steadily increased between St 20 and 50. For each stage, between 2–10 sections were examined. **, $p < 0.001$ vs St. 50; *, $p < 0.05$ vs. St. 50. Scale bars: 50 lm in **A**, **B**, **D**, **E, F, G, H** and **I**.

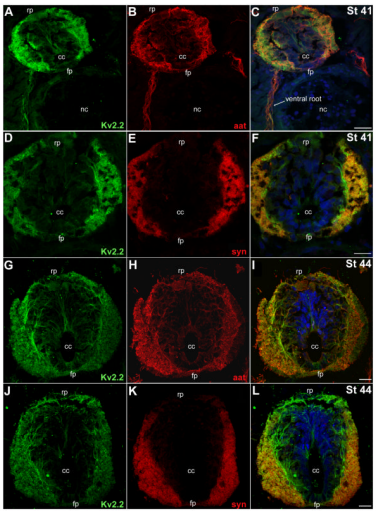

Fig. 3.

In the spinal cord, acetylated α-tubulin and syntaxin colocalized with the majority of Kv2.2 immunolabeling. Transverse cryostat (18 μm) sections were incubated with the Kv2.2 antibody and the acetylated α-tubulin (aat) or syntaxin (syn) monoclonal antibodies. In the merged images of Panels **C**, **F**, **I** and **L**, the Hoechst counterstain is shown (blue). **A, B, C**: At St 41, Kv2.2 (**A**, green) and aat (**B**, red) were both present in the lateral regions of the spinal cord, as well as in peripheral motor axons in the ventral roots (**C**, arrow). A merged image (**C**) highlights the close apposition of Kv2.2 immunolabeling to that of aat. **D, E, F**: At St 41, Kv2.2 (**D**, green) and syn (**E**, red) predominated in lateral regions of the spinal cord. Syn labeling (**E**) was more restricted to the lateral margins while Kv2.2 immunolabeling was detected dorsally near the roof plate (rp) as well as processes surrounding medial portions of the cord (**F**). **G, H, I**: At St 44, Kv2.2 (**G**, green) and aat (**H**, red) persisted in lateral regions of the spinal cord. However, in comparison to St 41 (**A**, **B**, **C**) Kv2.2 (**G**, green) and aat (**H**, red) were now present in more medial regions and continued to show extensive colocalization. **J, K, L**: At St 44, Kv2.2 (**J**, green) and syn (**K**, red) persisted together in lateral spinal cord, but Kv2.2 protein was also detected without syn in more medial regions (**L**). Scale bars: 20 lm in all panels. cc, central canal; fp, floor plate; nc, notocord; rp, roof plate.

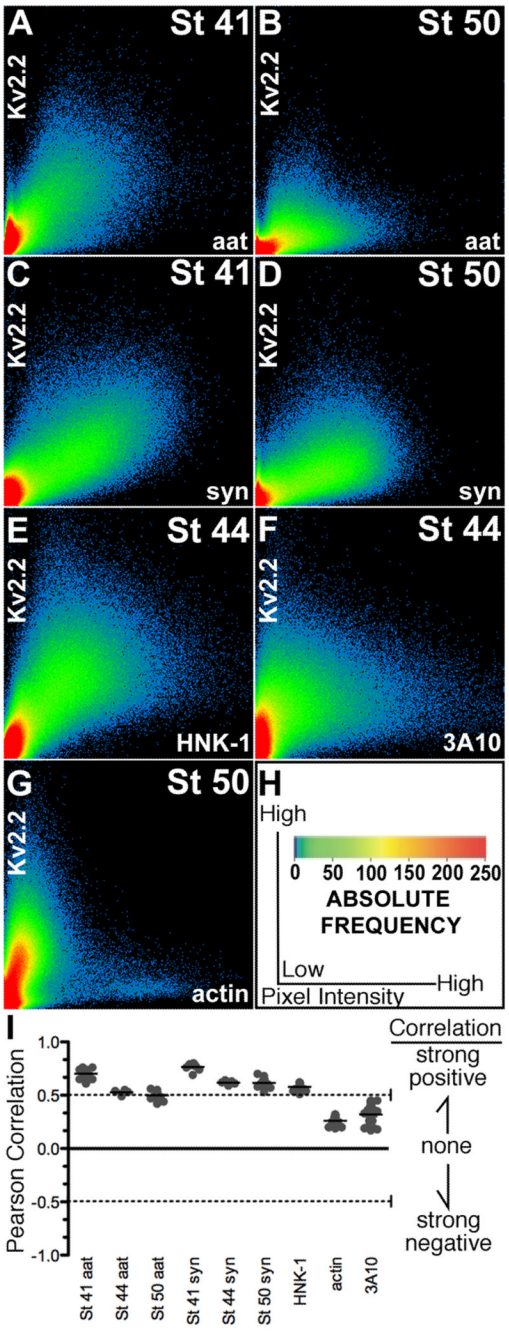

Fig. 4.

The intensity of Kv2.2 immunofluorescence in the spinal cord correlated with those of some but not all markers examined. **A** – **G:** For individual confocal sections, we constructed scatter plots that showed, for each pixel, the intensity of Kv2.2 immunofluorescence (y-axis) and that of the marker being compared (x-axis): aat (A, St 41; B, St 50), syn (C, St 41; D, St 50), HNK-1 (E, St 44), 3A10 (F, St 44) and actin (G, St 50). The frequency of each combination of Kv2.2 and marker fluoresence intensities is indicated in pseudocolor (**H**). I: Pearson correlation coefficients indicated colocalization between Kv2.2 and aat, syn and HNK-1, but not 3A10 or actin.

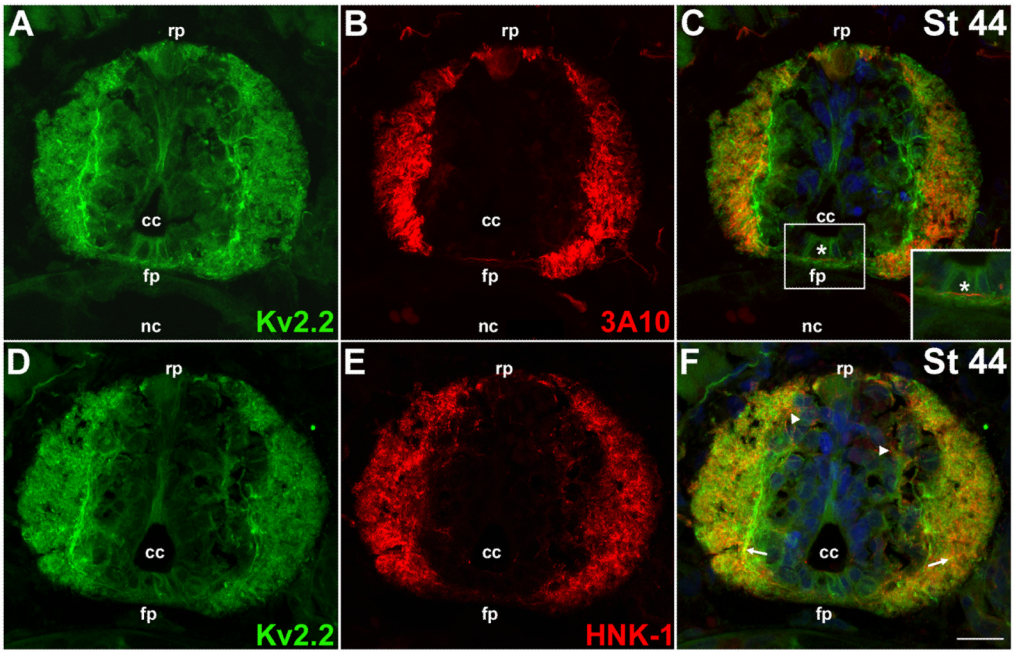

Fig. 5.

In the developing spinal cord, 3A10 and HNK-1 colocalize, to an extent, with the Kv2.2 immunolabeling. Transverse cryostat (18 μm) sections were incubated with the Kv2.2 antibody and 3A10 or HNK-1 mouse monoclonal antibodies. Antibody labelings were detected using goat anti-rabbit Alexa 488 (green; Kv2.2) and goat anti-mouse Alexa 568 (red) secondary antibodies. Sections were counterstained with Hoechst (blue). **A, B, C:** At St 44, Kv2.2 (**A**, green) was detected in lateral portions of the spinal cord that contain developing neuronal processes. 3A10 (**B**, red), a marker of commissural interneurons, showed a more restricted expression in lateral spinal cord in comparison to Kv2.2 (**C**). Moreover, crossing axons (asterisks, inset) that were 3A10 positive did not also show Kv2.2 immunoreactivity. **D, E, F:** At St 44, Kv2.2 (**D**, green) and HNK-1, (**E**, red) a marker for glycosylated neural cell adhesion molecules, predominated in lateral regions of the spinal cord and also decorated the plasma membranes of neuronal cell bodies. HNK-1 labeling appeared by itself (**F**, arrowheads) as well as colocalized with Kv2.2 immunoreactivity (**F**, arrows) in the medial cell body region. Scale bar: 20 μm for all panels. cc, central canal; fp, floor plate; nc, notocord; rp, roof plate.

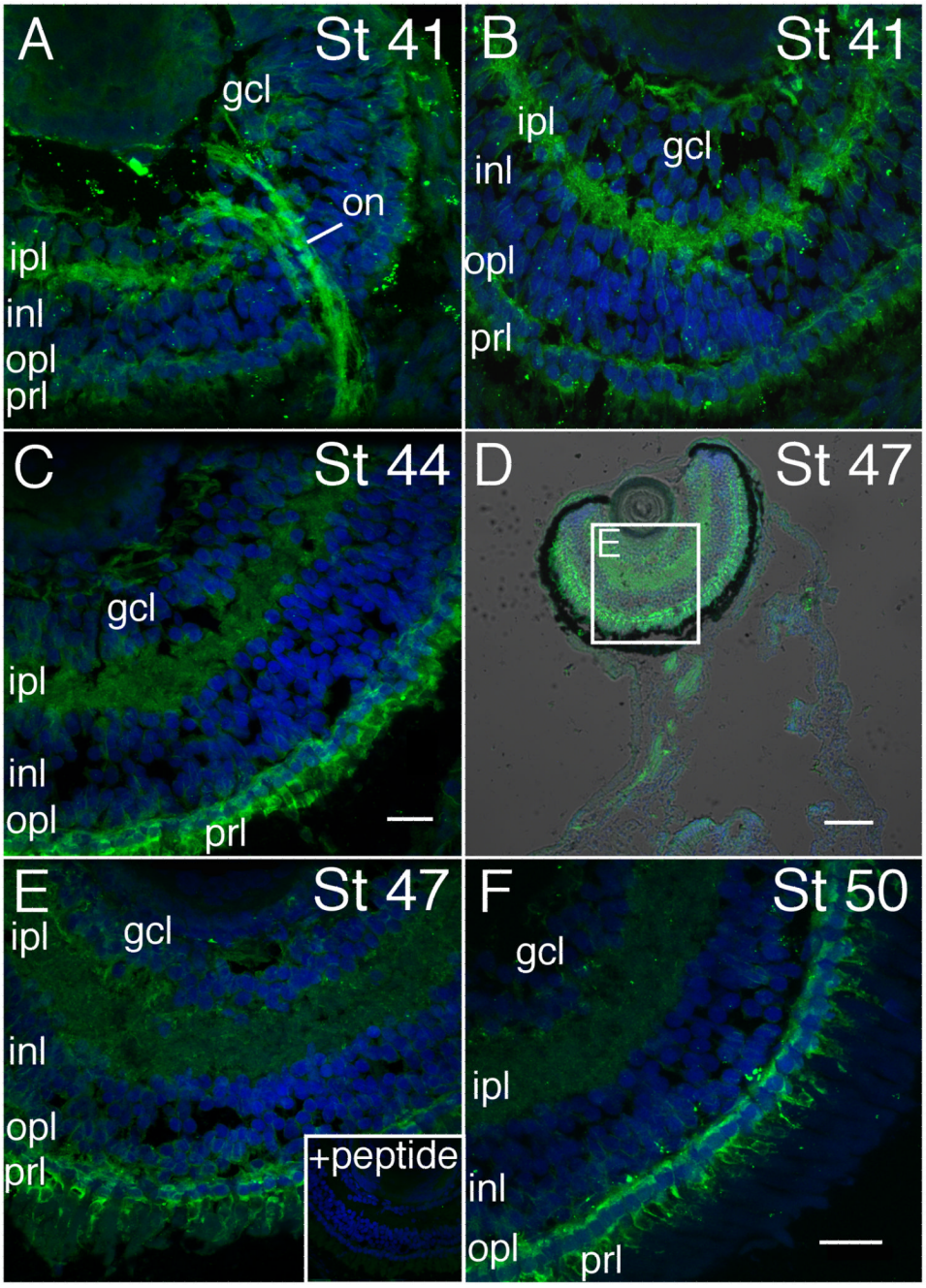

Fig. 6.

Kv2.2 protein was present early in the developing retina. Transverse cryostat (18 μm) sections were incubated with the Kv2.2 antibody or pre-blocked Kv2.2 antibody (inset in **E**). Sections were counterstained with Hoechst (blue). **A, B**: In the retina of St 41 embryos, Kv2.2 immunoreactivity localized to the inner and outer plexiform layers (ipl, opl), axons in the ganglion cell layer (gcl), and somata of the photoreceptor layer (prl). Kv2.2 was also present in the optic nerve (on) and occasional cell bodies and processes within the inner nuclear layer (inl). **C**: In the St 44 retina, Kv2.2 protein was present in the ganglion cell layer, the inner and outer plexiform layers, photoreceptor layer somata, and a subset of somata and processes within the inner nuclear layer. **D, E**: In the St 47 retina, Kv2.2 protein

showed a similar distribution as found at St 44. **E, Inset**: Pre-incubation of the Kv2.2 antibody with Kv2.2 peptide blocked the immunoreactive signal. **F**: In the stage 50 retina, the Kv2.2 protein displayed less intense immunoreactivity in the inner plexiform and ganglion cell layers in comparison to previous stages. In other regions, the pattern of immunolabeling was similar to that of earlier stages. Scale Bars: 20 μm in **A**, **B**, **C**, **E** and F; 200 μm in **D**. gcl; ganglon cell layer; inl, inner nuclear layer; ipl, inner plexiform layer; on, optic nerve; opl, outer plexiform layer; prl, photoreceptor layer.

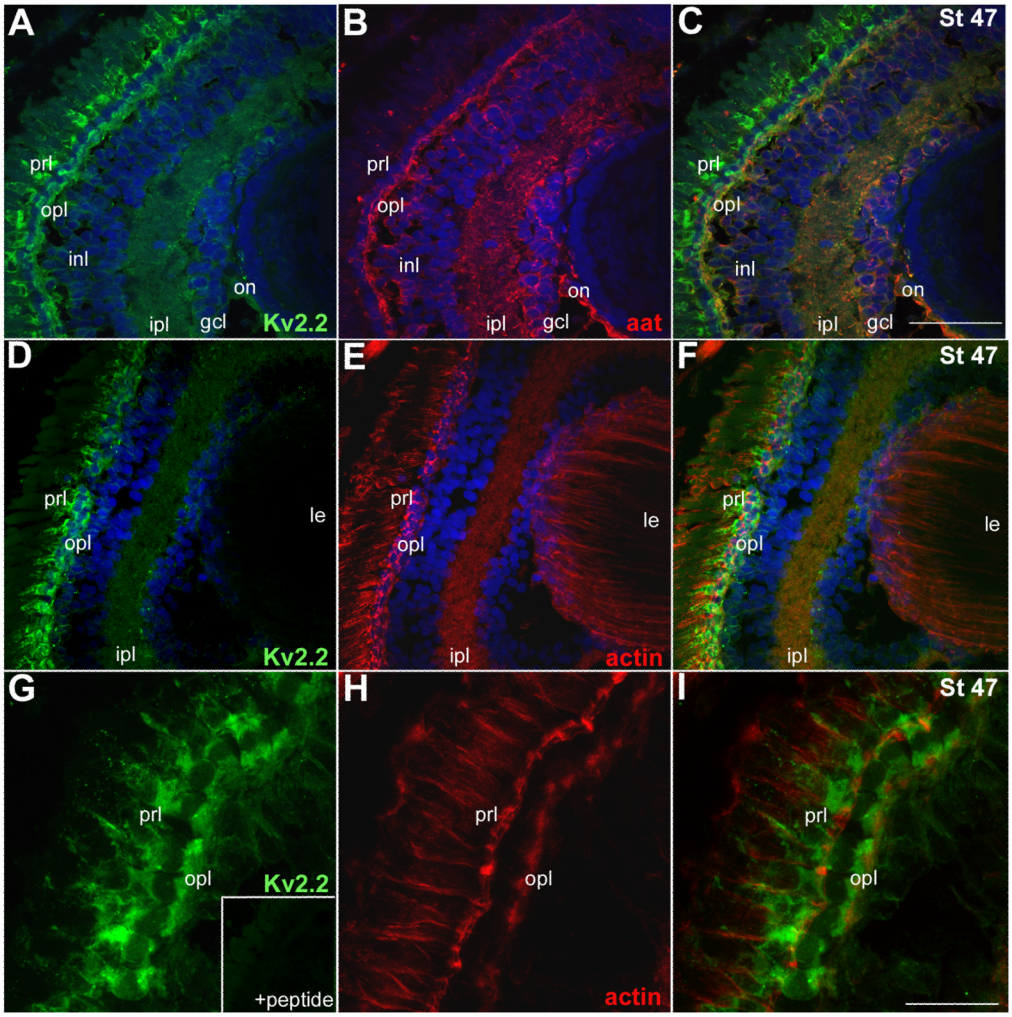

Fig. 7.

In the retina, Kv2.2 immunolabeling colocalized with α-tubulin but not F-actin. Transverse cryostat (18 μm) sections were incubated with the Kv2.2 antibody or pre-blocked Kv2.2 antibody (insert in **G**) and aat mouse monoclonal or fluorescently labeled-phalloidin to detect F-actin. In some sections, nuclei were counterstained with Hoechst (**A**–**F**, blue). **A, B, C**: At St 47, Kv2.2 (**A**, green) was abundant in synaptic layers (opl, ipl) and the cell bodies of the photoreceptor layer (prl). Less abundant labeling was also detected within the inner nuclear layer (inl) and ganglion cell layers (gcl). aat (**B**, red) localized to the inner and outer plexiform layers, the inner nuclear layer, the ganglion cell layer and optic nerve (on). A merged image (**C**) illustrates the close apposition of aat and Kv2.2 immunolabeling, specifically in the inner and outer plexiform, inner nuclear, and ganglion cell layers. **D, E, F**: At St 47, Kv2.2 (**D**, green) was present in the photoreceptor layer and both the inner and outer plexiform layers. F-actin (**E**, red) was present in the photoreceptor layer, inner and outer plexiform layers, and the lens. **F**: In contrast to aat (**C**), F-actin did not colocalize extensively with Kv2.2. Although Kv2.2 and F-actin were both present in the inner and outer plexiform layers, their labeling patterns showed only occasional overlap in the merged image (**F**). Scale Bar (**C**): 50 μm for **A–F. G, H, I**: A magnified view of the St 47 photoreceptor layer indicated that Kv2.2 (**G**, green) was detected in the cell bodies of photoreceptor cells and the outer plexiform layer. Inset: Preincubation of the Kv2.2 antibody

with the Kv2.2 peptide block effectively eliminated Kv2.2 immunolabeling. F-actin (**H**, red) was present in both the inner and outer segments of the photoreceptor cell, as well as the outer plexiform layer. A merged image (**I**) demonstrated that in some regions, notably the outer plexiform layer, Kv2.2 and actin were adjacent to each other. In photoreceptor cells, the majority of Kv2.2 protein and F-actin were detected in different locations. Scale Bar (**I**) 50 μm for **G–I**. gcl, ganglion cell layer; inl, inner nuclear layer; ipl, inner plexiform layer; le, lens; opl, outer plexiform layer; prl, photoreceptor layer.

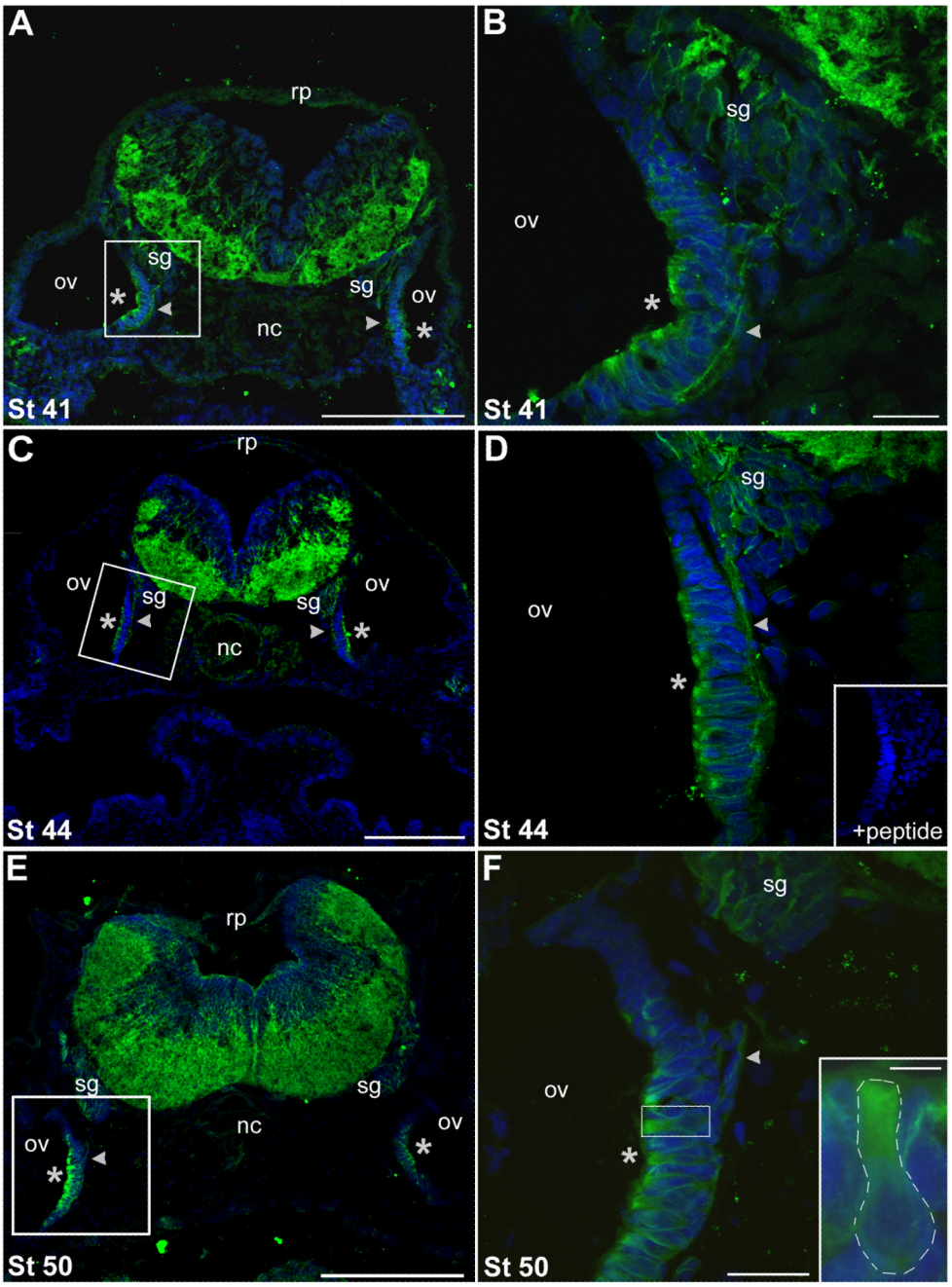

Fig. 8.

Kv2.2 protein was detected in the developing otic vesicle and the hindbrain. Transverse cryostat (18 μm) sections were incubated with the Kv2.2 antibody or pre-blocked Kv2.2 antibody (inset, **D**). Sections were counterstained with Hoechst (blue). **A**: At St 41, Kv2.2 immunoreactivity was present in the ventral lateral hindbrain and the medial epithelium of the otic vesicle (asterisk), where the sacculus forms. **B**: A magnified image of the boxed area in (**A**) illustrates the localization of Kv2.2 protein to the medial side of the otic epithelium. Kv2.2 protein was also detected in the innervating nerve (arrowhead) and the spiral ganglion cells (sg). **C**: At St 44, the Kv2.2 immunolabeling in the hindbrain had expanded both dorsally and medially. Kv2.2 protein was again detected in the saccular portion of the otic

epithelium. **D**: A magnified view of the boxed area in (**C**) shows Kv2.2 protein again at the medial side of the otic epithelium. Also, Kv2.2 immunolabeling persisted in the innervating nerve and the spiral ganglion cells. Inset: Preincubation of the Kv2.2 antibody with the Kv2.2 peptide block effectively eliminated Kv2.2 immunolabeling. **E**: At St 50, Kv2.2 protein expression had continued both dorsal and medial expansion in the hindbrain. The Kv2.2 immunolabeling in the otic epithelium was again present. **F**: A magnified view of the boxed area in (**D**) illustrates a strong Kv2.2 presence in the otic epithelium, as well as the spiral ganglion cells and innervating nerve. In the inset, Kv2.2 immunolabeling is detected around the membrane of the developing hair cell, with large cytosolic portions of the protein evident towards the apical portion of the soma. Scale bars (**A**, **C**, **E**): 200 μm; (**B**, **D**, **F**): 20 μm; inset (**F**): 5 lm. nc, notochord; ov, otic vesicle; rp, roof plate; sg, spiral ganglion.

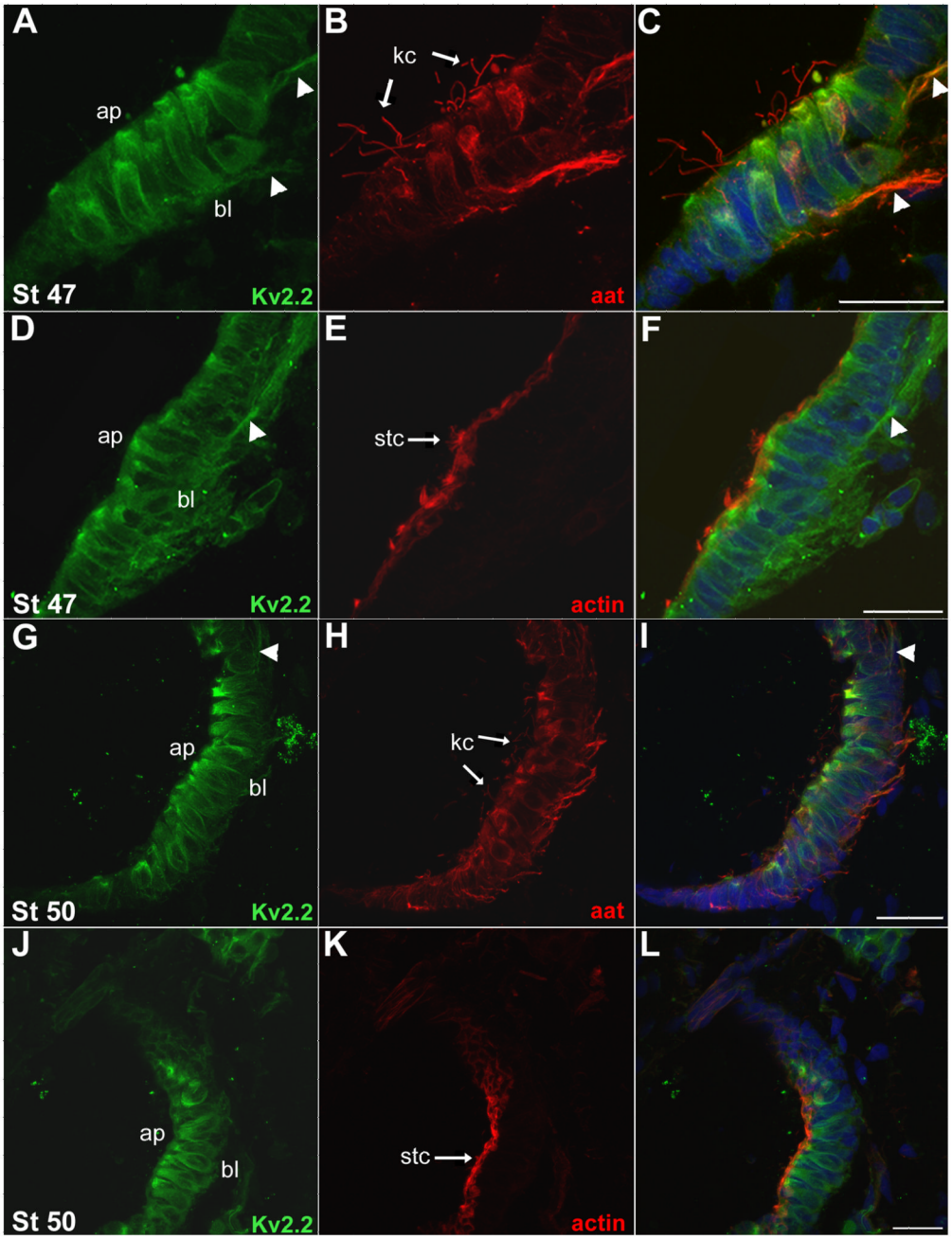

Fig. 9.

In the otic vesicle, Kv2.2 was present at the apical end of hair cells. Transverse cryostat (18 μm) sections were incubated with the Kv2.2 antibody and aat monoclonal or fluorescently labeled-phalloidin. Sections were counterstained with Hoechst (blue). **A**, **B**, **C**: At St 47 Kv2.2 (**A**, green) was abundant in the otic epithelium, at the apical side (ap) of developing hair cells. Kv2.2 was also present along the long axis of the hair cells flanking the soma, and along the innervating nerve (arrowheads). aat (**B**, red) marked the kinocilia of the hair cells, as well as the innervating nerve and portions of the soma. A merged image (**C**) illustrates the localization of the Kv2.2 protein at the base of the kinocilia at the apical end of the hair cells. Kv2.2 and aat colocalized in the innervating nerve. **D**, **E**, **F**: At St 47, Kv2.2 (**D**, green)

continued to be present apically, along the long-axis of hair cells, and in the innervating nerve. F-actin (**E**, red) was present in the hair cell stereocilia. A merged image (**F**) demonstrates the localization of the Kv2.2 immunolabeling at the base of the actin-containing stereocilia. **G**, **H**, **I**: At St 50, Kv2.2 immunolabeling (**G**, green) persisted at the apical side of the hair cells and along the long axis flanking the soma. aat (H, red) marked the hair cell kinocilia and the innervating nerve. A merged image (**I**) shows strong Kv2.2 immunolabeling at the base of kinocilia. **J**, **K**, **L**: At St 50 Kv2.2 immunolabeling (**J**, green) was detected in the apical portion of hair cells. F-actin (**K**, red) marked the hair cell stereocilia. A merged image (**L**) displays the localization of Kv2.2 protein at the base of the stereocilia. Scale bars (**A**–**L**): 20 μm. ap, apical membrane; bl, basolateral membrane; kc, kinocilium; stc, stereocilia.

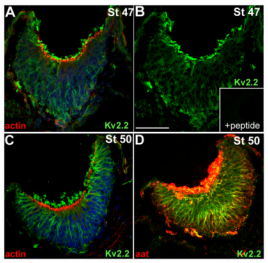

Fig. 10.

Kv2.2 immunoreactivity was present in the developing olfactory system. Transverse cryostat (18 μm) sections were incubated with the Kv2.2 antibody or peptide-blocked Kv2.2 antibody (inset in **B**) and aat or fluorescently-labeled phalloidin to detect F-actin. Sections were counterstained with Hoechst (blue in Panels **A** and **C**). **A**: At St 47, Kv2.2 (green) was present in the developing nares, throughout the dense cellular layer and distally near the principal cavity (asterisk). F-actin (red) was present in the microvilli, proximal to the Kv2.2-imunolabeling near the principal cavity (*). **B**: A peptide block (inset) effectively eliminated Kv2.2 immunolabeling present in the St 47 retina. **C**: At St 50, Kv2.2 (green) immunolabeling in the developing nares was similar but stronger to that observed at St 47. **D**: At St 50, aat (red) localized to the cilia and ventral portions of the cellular area of the nares. As was true in other tissues, Kv2.2 (green) colocalized with aat (yellow) in the cilia and cellular region. Scale bar: 50 μm for **A–D**.

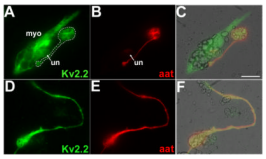

Fig. 11.

In culture, Kv2.2 protein colocalized with α-tubulin and was present in long processes. In cultured cells, Kv2.2 immunolabeling was detected in neuronal cell bodies and axons, as well as in myocytes and undifferentiated cells. Cells were cultured from dissociated neural plates of St 15–17 *Xenopus* embryos. Cultures were incubated with the Kv2.2 and aat antibodies. **A, B, C:** Kv2.2 (**A**, green) was present in a myocyte (myo), an undifferentiated cell (un), and a neuron (white outline). The Kv2.2 protein was found in the cell body, process, and terminal of the differentiated neuron (white outline). aat (**B**, red) localized to the cell body, process and terminal of the neuron; the terminal contacted the myocyte. A merged image (**C**) supported colocalization of Kv2.2 and aat immunolabeling in the neuronal cell body, process, and terminal. **D, E, F:** Kv2.2 (**D**, green) was present in the cell body and long process of a differentiated neuron. aat (**E**, red) was also detected in the cell body and long process of the neuron. A merged image (**F**) demonstrated strong colocalization of Kv2.2 and aat immunolabeling. Scale bar (**C**): 20μm in A–F.

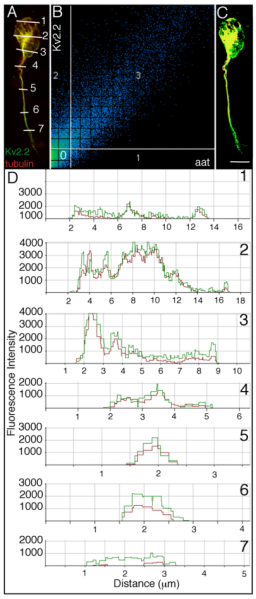

Fig. 12.

In culture, a majority of Kv2.2 protein colocalized with α-tubulin. Neurons in culture were fixed, immunolabeled for Kv2.2 (green) and aat (red), and imaged using confocal microscopy. **A**: Kv2.2 (green) and aat (red) immunolabeling were present in the long process and cell body of a neuron in culture. **B**: For the image in A, a scatter plot showed the intensity of Kv2.2 immunofluorescence (y-axis) and that of aat immunofluorescence (x-axis) for each pixel. The lower left hand corner (region 0) contains pixels that were excluded in the analysis because they were below threshold (background) levels. On the basis of the Kv2.2 and aat immunofluorescence intensities, the remainder of the pixels are grouped into one of three regions: 1, aat immunofluorescent with little to no Kv2.2 immunofluorescence; 2, Kv2.2 immunofluorescent with little to no aat immunofluorescence; 3, immunofluorescent for both Kv2.2 and aat. **C**: The neuron shown in A is presented as a masked image according to regions in Panel B: region 1(green), region 2 (red), region 3 (yellow). Scale Bar: 10μm. D: For the individual lines drawn through the neuron in Panel A, profiles of the Kv2.2 and aat immunofluorescence intensities as a function of distance are plotted. In each case, the aat signal either followed closely the Kv2.2 signal or was not present.

Table I

Primary Antibody/Toxin Information

Agent	Source(Catalogue/Lot #)	Dilution	Source
acetylated α-tubulin mouse mab[1]	Sigma[2] (T6973/017K4845)	1:1000	cytoskeletal marker for tubulin; generated in mice against *Strongylocentrotus purpuratus*(seaurchin) acetylated α-tubulin; in immunoblot, recognizes acetylated α-tubulin in human, pig, bovine, rat, hamster, monkey, chicken and frog(Piperno and Fuller, 1985; Chu and Klymkowsky, 1989
Phalloidin *Amanita* toxin	Molecular Probes[3] (O7466/41B1–2)	1:30	cytoskeletal marker for F-actin; conjugated to Oregon Green 488
Syntaxin mouse mab[1]	Sigma[2](S0664/026K4851)	1:1000	synaptic vesicle marker (Manzini et al., 2007); generated in mice against a synaptosomal plasma- membrane fraction prepared from adult rat hippocampus; recognizes a single band of ~35 KDa in immunoblot.
Kv2.2 rabbit polyclonal	Phosphosolutions[4] (1002-KV22/736)	1:100	generated in rabbits against a 26-amino acid peptide within the carboxyl-terminus of Kv2.2 (see Materials and Methods; Fig. 1, immunoblot; Fig. 2, pre-absorption control)
3A10 mouse mab[1]	DSHB[5](3A10c/021704)	1:25	generated in mice against chicken nervous tissue; recognizes a neurofilament-associated antigen in *Xenopus* commissural interneurons (Robles and Gomez, 2006)
HNK-1 mouse mab[1]	Sigma[2](C0678/128H4870)	1:200	generated in mice against unfixed homogenate of cat primary visual cortex; recognizes myelin associated glycoprotein, a high weight chondroitin sulphate proteoglycan, and145 and 170 kDa high molecular weight integral membrane forms of neural cell adhesion molecule (Nordlander, 1993)

[1] mab: monoclonal

[2] Sigma-Aldrich Co., St. Louis, Mo.

[3] Molecular Probes-Invitrogen, Carlsbad, Ca.

[4] Phosphosolutions, Aurora, Co.

[5] Developmental Studies Hybridoma Bank. The 3A10 monoclonal antibody developed by Drs. T. Jessell and J. Dodd was obtained from the Developmental Studies Hybridoma Bank developed under the auspices of the NICHD and maintained by The University of Iowa, Department of Biological Sciences, Iowa City, IA 52242.